LAWRENCE
LIVERMORE
NATIONAL
LABORATORY

LLNL-JRNL-400730

Evaluation of Forecasted Southeast Pacific Stratocumulus in the NCAR, GFDL and ECMWF Models

C. Hannay, D. L. Williamson, J. J. Hack, J. T. Kiehl, J. G. Olson, S. A. Klein, C. S. Bretherton, M. Köhler

January 25, 2008

Journal of Climate

Disclaimer

Evaluation of Forecasted Southeast Pacific Stratocumulus in the NCAR, GFDL and ECMWF Models.

Cécile Hannay, David L Williamson, James J Hack, Jeffrey T Kiehl, Jerry G Olson,

National Center for Atmospheric Research, Boulder, Colorado*

Stephen A. Klein,

Lawrence Livermore National Laboratory, Livermore, California

Christopher S Bretherton,

Department of Atmospheric Sciences, University of Washington, Seattle, Washington.

and Martin Köhler

European Center for Medium-range Weather Forecasts, Reading, England

---

* The National Center for Atmospheric Research is sponsored by the National Science Foundation.

Corresponding author address: Cécile Hannay, National Center for Atmospheric Research, 1850 Table Mesa Drive, Boulder, CO 80305

E-mail: hannay@ucar.edu

Abstract

We examine forecasts of Southeast Pacific stratocumulus at 20S and 85W during the East Pacific Investigation of Climate (EPIC) cruise of October 2001 with the ECMWF model, the Atmospheric Model (AM) from GFDL, the Community Atmosphere Model (CAM) from NCAR, and the CAM with a revised atmospheric boundary layer formulation from the University of Washington (CAM-UW). The forecasts are initialized from ECMWF analyses and each model is run for 3 days to determine the differences with the EPIC field data.

Observations during the EPIC cruise show a stable and well-mixed boundary layer under a sharp inversion. The inversion height and the cloud layer have a strong and regular diurnal cycle. A key problem common to the four models is that the forecasted planetary boundary layer (PBL) height is too low when compared to EPIC observations. All the models produce a strong diurnal cycle in the Liquid Water Path (LWP) but there are large differences in the amplitude and the phase compared to the EPIC observations. This, in turn, affects the radiative fluxes at the surface. There is a large spread in the surface energy budget terms amongst the models and large discrepancies with observational estimates.

Single Column Model (SCM) experiments with the CAM show that the vertical pressure velocity has a large impact on the PBL height and LWP. Both the amplitude of the vertical pressure velocity field and its vertical structure play a significant role in the collapse or the maintenance of the PBL.

1. Introduction

Stratocumulus clouds strongly influence the global climate due to their radiative effects. These clouds form over oceans with cold sea surface temperature (SST). They form at the top of the planetary boundary layer (PBL) and are capped by a sharp inversion of temperature and moisture (e.g, Klein and Hartmann, 1993). Due to their high reflectivity, stratocumulus clouds strongly decrease the solar radiation that reaches the surface. Also, due to their large optical thickness, they emit like a black body in the infrared. The net radiative effect is a strong cooling of the surface and the PBL with respect to clear skies. These radiative properties make stratocumulus a crucial factor in the surface energy balance so that their realistic simulation is important for climate modeling.

Stratocumulus have a diurnal cycle in the cloud amount and liquid water path (LWP) with an early morning maximum and an early afternoon minimum in both quantities (Wood et al., 2002). At night, the strong longwave cooling near the top of the cloud creates turbulence. This produces a well-mixed PBL, which transports moisture from the surface into the PBL and maintains the cloud. During daytime, in-cloud absorption of solar radiation largely compensates the longwave cooling. As a result, the turbulence decreases after sunrise and the cloud layer thins, due to the decoupling between the cloud and the surface. The diurnal cloud and LWP variations have a considerable effect upon the earth's radiation budget (e.g., Bergman and Salby, 1997) and it is therefore important that General Circulation Models (GCMs) simulate accurately the diurnal cycle of clouds. In the Southeast Pacific, the diurnal cycle of stratocumulus is very pronounced, and it is stronger than in other stratocumulus regions due to non-local effects (Rozendaal et al., 1995; Wood et al., 2002; Zuidema and Hartmann, 1995). Other mechanisms may amplify the stratocumulus diurnal cycle in the Southeast Pacific. In particular, the diurnal cycle in subsidence

has been found to play an important role in this region: it increases the amplitude of the diurnal cycle of the stratocumulus amount with respect to the cycle forced by radiation only (Garreaud et al., 2004).

Despite improvements in observing and understanding the stratocumulus regimes (e.g. Stevens et al., 2003; Bretherton et al., 2004), the cloud amount is usually underestimated in GCMs, even when the SSTs are observationally prescribed (Siebesma et al., 2004). As the stratocumulus regions have a significant cooling effect on the underlying ocean, an underestimation of the cloud amount causes an overestimation of the net heat surface flux into the ocean, which can lead to positive SST biases in coupled models. Moreover, serious model biases persist in the representation of the vertical structure of the stratocumulus regions and in the diurnal cycle of the cloud layer. Studies assessing the representation of stratocumulus off the coast of California (Duynkerke et al., 2004) and Southeast Pacific (Bretherton et al., 2004) showed that the PBL in climate models was typically too shallow in the GCMs compared with observations, while LWP was typically underestimated and its diurnal cycle poorly represented.

Understanding the causes of the stratocumulus bias in climate simulations is difficult because of the complexity and non-linear interactions of the processes maintaining the cloud. In-situ observations, which are only available for limited periods of time, are difficult to compare with model climatological statistics to evaluate parameterization performance. Applying GCMs in short-term forecasts can be extremely valuable because it minimizes the interaction of large non-linear systematic model errors that grow over time, and because forecasts can be evaluated over limited observation periods. The forecast approach is described in (Phillips et al., 2004) and it has been successfully used in several studies (Williamson et al., 2005; Boyle et al., 2005; Klein et al., 2006; Williamson and Olson, 2007). The principle of the method is that if the model is initialized realistically, the systematic errors in short forecasts are predominantly due to

parameterization errors. That is because the large-scale circulation is strongly controlled by the initial conditions and stays close to the observed state in these short-range runs. Therefore, it is possible to gain insight into the parameterization deficiencies and to diagnose the processes behind the drift away from reality.

Here, we examine the way three climate models and one analysis system represent a region of persistent stratocumulus in global forecasts examined at a column in the Southeast Pacific (20S-85W). This column is well suited for such a study because of the availability of observational datasets to evaluate the forecasts: the 2001 East Pacific Investigation of Climate (EPIC) cruise provides a 6-day comprehensive observational dataset at this location including surface measurements and remote sensing (Bretherton et al., 2004).

In section 2 we describe the models, the observational datasets and the forecast experiment settings. In section 3 we consider the forecast results with special attention given to the diurnal cycle. In section 4 we discuss some reasons why the forecasted PBL is low compared to observations. Finally we summarize our conclusions in section 5.

2. Data and model descriptions

2.1. Models

The models used in this study are the European Center for Medium-range Weather Forecasts (ECMWF) model cycle 29r1, the Atmospheric Model version 2 (AM) developed at the Geophysical Fluid Dynamics Laboratory (GFDL), the Community Atmosphere Model version

3.1 (CAM) developed at the National Center for Atmospheric Research (NCAR), and the Community Atmospheric Model with the University of Washington PBL/Shallow convection scheme (CAM-UW). The physical parameterizations of the models are summarized in Table 1. More details about the models can be found in Collins et al. (2004) for CAM, in GFDL Global Atmospheric Model Development Team (2004) for AM, in Bretherton and Park (2008) and Park and Bretherton (2008) for CAM-UW and in Tompkins et al. (2004) and Köhler (2005) for the ECWMF model.

The resolutions of the models are summarized in Table 2. The three GCMs (CAM, CAM-UW and AM) use a horizontal grid interval of about 200-300 km near the EPIC point while the ECMWF uses a much finer horizontal resolution (~40km). The vertical resolution ranges from 24 vertical levels for AM to 60 levels for the ECWMF model. Table 2 also compares the number of levels in the lowest 1.5 km above the surface. It shows that the model vertical grids only grossly resolve the PBL, which is one of the reasons commonly proposed to explain why models have difficulties reproducing stratocumulus. For instance, CAM at the standard 26-level vertical resolution has only 4 levels in the lowest 1.5 km of the model. Notice that CAM has 26 vertical levels in the climate runs while the forecasts runs were performed at two vertical resolutions: 30 and 60 levels. The 26-level configuration is the standard CAM vertical resolution for conducting global climate simulations. This configuration produces state of the art climate simulations (Boville et al., 2006; Collins et al., 2006; Hack et al., 2006). This is not the case for the 30-level and 60-level versions of CAM because the parameterizations are sensitive to the vertical resolution and the climate simulations are degraded at these vertical resolutions. However, the processes involved in the generation of these climatological errors have long timescales associated with them and they do not affect adversely the short-term forecasts. This implies that it is possible to either use a vertical resolution of 30 or 60 levels for the forecast experiments, and

therefore to increase the number of levels in the PBL and to match the vertical resolution of CAM-UW and ECWMF model. Here, we show the 30-level forecasts unless stated otherwise.

2.2. Observations, analyses and climatologies at the EPIC point (20S-85W)

In this study, we focus on an atmospheric column located at 20S-85W in a region of persistent stratocumulus of the Southeast Pacific approximately 700 km off the Peruvian/Chilean border (see Figure 1). This location is referred to hereafter as the 'EPIC point' or the 'EPIC column'. We employ a set of observations to assess the forecasts. The 2001 EPIC cruise provides a comprehensive dataset of remote sensing and surface measurements at the EPIC point for the period October 16-21, 2001 (Bretherton et al., 2004; Caldwell et al., 2005). Profiles of temperature and moisture were obtained from 3-hourly radiosonde observations. Surface sensible and latent heat fluxes were derived from temperature and humidity measurements taken on the ship instrumented tower using the bulk algorithm described by Fairall (1996). The LWP was derived from microwave radiometer brightness temperature measurements (Zuidema et al., 2005). The surface shortwave and longwave downwelling fluxes were obtained from shipboard radiometers. The 6-day observation period from the EPIC cruise reveals a well-mixed boundary layer capped by a stratocumulus layer just under a strong inversion. A marked diurnal cycle was observed, with a thicker cloud layer in early morning and a thinner one in early afternoon. The EPIC observations are extensively discussed in Bretherton et al. (2004).

We evaluate how well the models used here represent the features of the PBL and cloud layer at the EPIC point by comparing ECWMF analyses and AM, CAM and CAM-UW climatologies with observations. Figure 2 compares the 6-day observed mean profiles of water vapor and cloud liquid water with the mean from the ECMWF analysis for the same period and

with October climatologies from the 3 GCMs. The 6-day period is representative of typical October conditions in this area (Bretherton et al., 2004). In particular, there is good agreement between the PBL measured during the 2001 cruise and other estimations of the October PBL depth at the EPIC point. The diurnal average of the PBL depth at the EPIC point during the 2001 cruise was 1270 meters. Wood and Bretherton (2004) estimated a PBL depth of 1140 ± 100m for September-October 2000 using observed SSTs from the Tropical Rainfall Measuring Mission (TRMM) and cloud top temperatures from the Moderate Resolution Imaging Spectroradiometer (MODIS). Ahlgrimm and Randall (2006) derived a mean PBL depth of 1450 m from satellite-base Geoscience Laser Altimeter (GLAS) for October 2003. As the agreement of the satellite derived PBL depths and the PBL measured during the cruise is good, a comparison of October climatologies with the 6-day observations is relevant to indicate the climate bias at the EPIC point. In Figure 2, the ECWMF analysis qualitatively reproduces well the main features of the water vapor and cloud water profiles: the analysis simulates a well-mixed PBL under a marked inversion, and the cloud is fairly well represented. Quantitatively, the analysis produces a PBL which is too shallow by about 200 meters and too moist by 1 g kg^{-1}. The 3 GCMs produce PBLs, which are too shallow and the inversion is not well represented. This is especially the case for CAM, partly due to the poor vertical resolution (4 levels into the lowest 1.5km as shown in Table 2). The 3 GCMs underestimate the cloud liquid water, particularly the AM. The CAM places the cloud very close to the surface. The CAM-UW produces a significant improvement in the representation of the PBL and cloud layer at the EPIC point compared to CAM. The 2 versions differ only by the PBL/shallow convective scheme (see Table 1).

2.3 Forecast runs

Forecasts are initialized from the ECWMF analysis created by cycle 29r1, which covers the period October 11-22, 2001. This state of the art analysis consists of the ECMWF cycle 28r4 plus a new stratocumulus PBL parameterization (Köhler, 2005) which became cycle 29r1. The main aim in upgrading the PBL parameterization was to improve low-level cloudiness and pave the way towards the unification of the PBL and shallow convection schemes. The PBL is too shallow in the analysis compared to observations, as shown in Figure 2. However, this bias is worse in other analyses that we might have used as initial conditions, such as the ERA40 reanalysis (Uppala, 2005), the NCEP operational analysis or the Japanese 25-year Reanalysis (Onogi et al., 2007). At the moment, the ECWMF analysis cycle 29r1 is the most accurate dataset from which to initialize the forecasts for this location. The initialization includes the temperature, specific humidity, horizontal winds and surface pressure fields. These fields are carefully interpolated to each model native grid. Forecasts are started every day at 12Z for the period October 11-22, 2001 and run for a 3-day period. The forecast data are saved hourly with instantaneous values for state variables and time-average values for fluxes and forcing terms. The CAM, CAM-UW and AM forecasts are interpolated to the EPIC point using the distance-weighted average from the 4 closest model gridpoints, while the ECMWF forecasts save the closest model point (84.96 W and 19.84 S). Notice that using a weighted average versus looking at the closest model column gives qualitatively similar results for most variables. On one hand, the 4 model gridpoints bracketing the EPIC point in the GCMs show a relatively homogeneous behavior. On the other hand, averaging the ECWMF forecasts over a domain size comparable to the GCMs gridbox gives results qualitatively similar to extracting the closest column output.

To reduce the noise and to better show forecast systematic errors, we examine the average over the forecasts at fixed elapsed times as illustrated in Figure 3. We refer to this average as the 'ensemble mean forecast'. Results from the 3rd day of the forecasts (hour 48-72) are emphasized for reasons discussed in section 3. In particular, we examine here the ensemble

mean forecast time-averaged over the 3rd day (hours 48-72), which will be referred as 'the daily average of the ensemble mean forecast' or 'the ensemble mean daily average'. We also examine the diurnal cycle of the ensemble mean forecast over the 3rd day (hours 48-72), which will be referred as 'the diurnal cycle of the ensemble mean forecast' or 'the ensemble mean diurnal cycle'.

3. Forecasts at the EPIC point

3.1. Water vapor profiles

First we examine how the vertical structure of the moisture evolves in the forecasts and how the forecasts compare with model climatologies. Figure 4 shows the vertical profiles of the ensemble mean forecast specific humidity as a function of the forecast time (at day 0, day 1 and day 3). The forecasts at day 0 correspond to the initial condition from the ECWMF analysis interpolated to the model grid. The ECWMF model preserves the moisture characteristics throughout the 3-day forecasts. In CAM, the PBL (defined here as the base of the inversion in specific humidity) rapidly collapses from about 800 to 400 meters within 3 days of forecasts. The CAM-UW shows similar behavior although the collapse is somewhat less pronounced. The AM better maintains the PBL depth than CAM and CAM-UW; however, the sharpness of the inversion is reduced between day 0 and day 3. Note that the timescale in which the PBL height adjusts is consistent with Schubert et al. (1979) who demonstrated with a mixed-layer model of stratocumulus that the adjustment time scale of the PBL height is on the order of several days. Figure 4 also shows the mean October climatology at the EPIC point for the 3 GCMs. A climatology is not available for the version of the ECWMF model used here for forecasts. At this

location, the GCM forecast biases develops very quickly. Within the 3-day forecast, the forecast error qualitatively reproduces the climate bias: the inversion becomes more the diffuse in the GCMs and the PBL significantly shallows in CAM and in CAM-UW. The full climate error develops on a longer timescale with additional slower processes that come into play, but the forecast biases are clearly relevant to the climatological biases.

Previous studies showed that an enhancement of the vertical resolution in the boundary layer can lead to improvements in the vertical structure of the cloud-topped boundary layer produced by GCMs in both well-mixed and decoupled situations (e.g. Bushell and Martin, 1999; Pope et al., 2001). We investigated the impact of increased vertical resolution on the PBL depth and in particular whether a vertical resolution comparable to the ECMWF model can help to maintain the PBL depth in the CAM forecasts. Figure 4 shows the CAM forecast specific humidity as a function of forecast time with a 60-level vertical resolution. Increasing the vertical resolution from 30 to 60 levels has little impact on the PBL depth. At both resolutions, the PBL rapidly collapses from about 800 to 400 meters within 3 days into the forecast.

In the remainder of the section 3, we focus on results from the 3rd day of forecast (hour 48-72) because at that stage the PBL has shallowed significantly and most of the forecast error has developed, but the large-scale state has not yet diverged too far from the observations. In particular, in CAM, CAM-UW and ECMWF model, the diurnal cycle of the vertical velocity in the day 3 forecast looks the same as that in the day 1 forecast showing that the model dynamical state does not diverge too quickly from its initial state (not shown here). The AM shows more noise arising from the interpolation to the model grid in the early part of the forecasts, but there is no indication of the noise after day 2.

3.2. Energy balance at the surface

Achieving an accurate energy balance at the surface in climate models is important, especially when coupling atmospheric models with ocean models. The surface energy balance can be written:

$$\text{Net flux} = SW + LW + SH + LH$$

where SW and LW are the net shortwave and longwave radiative fluxes at the surface and SH and LH are the sensible and latent heat fluxes from the surface to the atmosphere respectively. Our sign convention is that the fluxes are positive when directed into the atmosphere. Stratocumulus clouds strongly affect the surface energy balance through their radiative properties. The LWP determines the first order of the cloud radiative impact: larger values of LWP tend to decrease the net shortwave and longwave radiation at the surface. The microphysical properties of clouds such as the effective radius (Re) strongly influence the cloud radiative properties. For a given cloud water content, the underestimation of the effective radius results in a corresponding increase of the optical depth and therefore shortwave cloud reflection. Here we examine how the models represent the energy balance terms, as well as the LWP and effective radius. We first concentrate the daily mean of these variables; then, we focus on their diurnal cycle.

Table 3 shows the daily average of the ensemble mean forecast (day 3) of the LWP and the surface energy budget terms as well as values of the cloud drop effective radius. The observed mean LWP is 106 g m^{-2}. It is underestimated in the 3 GCMs and overestimated in the ECMWF model. The deficit is very severe in the AM model, which has a mean value of 57 g m^{-2}. The effective radius estimated from MODIS measurements is about 17 microns at the EPIC point. A

computation of Re assuming an adiabatic layer cloud (Wood, 2006) and using the ship liquid water path with a cloud droplet number concentration of 100 cm^{-3} gives a value of 13 microns. These two estimates of Re have large uncertainties but are useful to compare with model values. The models use different formulations for the effective radius. The CAM and CAM-UW prescribe a constant effective radius but with different values over the ocean and land. Over the ocean, the effective radius is set to 14 microns in CAM and CAM-UW. The AM and the ECWMF model diagnoses the effective radius from the prognosed liquid water content and an assumed cloud droplet number concentration as described in Martin et al. (1994). The droplet number concentration over the ocean is set to 100 cm^{-3} in AM and 50 cm^{-3} in the ECWMF model. The insolation and extinction weighted effective radius is 6.7 microns for AM, and 12.4 microns for the ECWMF model. The AM effective radius is low compared to observations, whereas the CAM, CAM-UW, ECMWF models are consistent with the Re observations . The errors in LWP and effective radius affect the radiative fluxes at the surface and therefore, the surface energy balance. The CAM and CAM-UW overestimate the net longwave and shortwave radiative fluxes at the surface as a result of underestimating the LWP. The small values of the effective radius in AM are reflected in the net shortwave flux at the surface. There is a large spread in the components of the energy balance between the models and large discrepancies with observations.

We now examine how the models represent the diurnal cycle of these quantities. The cloud layer has a strong and regular diurnal cycle during the 6-day observation period (Bretherton et al., 2004). In the observations, the diurnal cycle of the LWP dominates the total variability: the range of the diurnal cycle of the LWP is around 150 g m^{-2} and it largely exceeds the day-to-day variation. For this reason, it is of interest to look at the diurnal cycle of LWP (Figure 5) and the cloud liquid water (Figure 6). Here, we compare the mean observed diurnal cycle with the diurnal cycle of the ensemble mean forecast for the same period. The observed LWP decreases after sunrise as the shortwave heating of the cloud increases, reaching a minimum in early afternoon,

around 1 pm local time (13 LT). Then the LWP increases and reaches a maximum in early morning, around 3 am local time (03 LT). It is interesting to notice that the minimum LWP during the 2001 cruise occurs a bit earlier than observed in other stratocumulus studies: satellite data and surface observations of stratocumulus have shown a minimum LWP occurring around 15LT (Rozendaal et al., 1995; Wood et al., 2002; Duynkerke et al., 2004). All the models capture a strong diurnal cycle in LWP but there are some differences in the amplitude and phase of the cycle. The ECWMF model reproduces fairly well the phase but the range is slightly too small and its mean daily value is overestimated. In CAM, the LWP reaches its minimum later than observations (around 14 LT) and is underestimated in the afternoon. In the CAM-UW and AM, the LWP falls close to zero in the late afternoon (16 LT). The AM dramatically underestimates the LWP during the night too. The cloud liquid water diurnal cycle shown in Figure 6 gives similar information to the LWP but it also gives an idea of the vertical extent of the cloud layer. The 4 models show a thick cloud layer which is lower than observations. The cloud layer breaks up in the late afternoon for CAM-UW and AM. Also, notice that for CAM the cloud water at forecast hour 72 (06 LT) does not match the cloud water at hour 48 (06 LT). The reason is that the PBL continues to collapse during the 3rd day of the forecast.

The scatter in LWP between models is reflected in the amount of downwelling shortwave radiation and net longwave radiation at the surface (see: Figure 5). The clouds tend to reduce the downward solar radiation and to a lesser extent the net longwave radiation at the surface. All the models overestimate the amount in downwelling shortwave reaching the surface in the afternoon. There are large discrepancies between models and observations in the net longwave at the surface. In particular, the CAM-UW and AM strongly overestimate the net longwave in the afternoon as expected from their LWPs.

The diurnal cycle of the latent and sensible heat fluxes is shown in Figure 5. The observed latent heat flux has a mean value of 98 W m^{-2} and the range of the mean diurnal cycle is about 25 W m^{-2}. All the models overestimate the latent heat fluxes with errors from 4 to 20% in the daily mean. The CAM and CAM-UW also overestimate the amplitude of the diurnal cycle. The AM shows a double maximum in the latent heat and there are large discrepancies in the phase of its diurnal cycle compared to observations. The observed sensible heat flux is much smaller than the latent heat with a mean value of 14 W m^{-2}. It exhibits a clear diurnal cycle with a range of about 6 W m^{-2} which is large compared its mean value. All the models overestimate the daily average of the sensible heat fluxes except the AM, which underestimates it. The amplitude of the diurnal cycle of sensible heat flux is typically overestimated compared to observations. The observed and modeled surface fluxes are estimated though the use of bulk aerodynamic formulas: SH $\sim U_r (T_s - T_a)$ and LH $\sim U_r \ (q_s - q_a)$ where U_r is the mean wind at some standard height (typically 10 m), T and q are the temperature and specific humidity respectively and the subscripts 's' and 'a' indicate values for the surface and the air at the reference level respectively. By looking at the terms of the bulk aerodynamic formulas, we can identify the source of the discrepancies in the turbulent fluxes. The discrepancies in the latent heat fluxes mainly correspond to discrepancies in the mean wind fields, while the discrepancies in the sensible heat can be related to discrepancies in the temperature difference between the surface and the air. For instance, the phase of the latent heat flux in AM is largely due to the wind field.

3.3. Vertical pressure velocity

We do not have observations of the vertical pressure velocity but it is instructive to compare the vertical velocity in the different models. The diurnal cycle of the ensemble mean forecast (day 3) of the pressure vertical velocity is shown in Figure 7. In the ECMWF model,

subsidence prevails during most of the day in the middle and lower troposphere. There is upward motion around midnight local time. Garreaud et al. (2004) showed that this upward motion was associated with a wave propagating from the Andes. This wave produces significant cooling and leads to a more turbulent PBL and more entrainment. This increases the amplitude of the diurnal cycle of the stratocumulus amount with respect to the cycle forced by radiation absorption only. The ECWMF model also produces a negative vertical velocity (upward motion) in the lower troposphere in the early afternoon between noon and 15 LT. The CAM and CAM-UW show a similar pattern to the ECMWF model above 800 mb but in the lower troposphere, the vertical velocity is different. In particular, the early afternoon upward motion is absent in CAM and CAM-UW. The AM shows a very different pattern of vertical motion with a strong maximum in the subsidence around 15 LT.

4. Discussion

In this section, we investigate the impact of the vertical velocity and its diurnal cycle on the PBL and cloud layer. In order to isolate the effect of the large-scale vertical velocity on the PBL and the cloud, we performed additional experiments using the Single Column Model of CAM (SCAM). The SCAM is a 1D version of CAM: it includes the same physics parameterization packages as CAM, but it is run over just one column with the resolved-scale tendency terms imposed (Hack and Pedretti, 2000; Hack et al., 2004). The SCAM is governed by prognostic equations for temperature, T and moisture, q:

$$\frac{\partial T}{\partial t} = -V \bullet \nabla T - \omega \left[\frac{\partial T}{\partial p} + \frac{RT}{pc_p} \right] + \mathrm{PAR}$$

$$\frac{\partial q}{\partial t} = -V \bullet \nabla q - \omega \frac{\partial q}{\partial p} + \mathrm{PAR}$$

where the left side terms of these equations represent the total tendency, the two first terms of the right side of the equations represent the tendency due to the resolved-scale advection (i.e. the sum of the horizontal and vertical advection) and PAR represents the subgrid scale parameterization term. The SCAM numerically integrates the equations for T and q starting from a prescribed initial condition and imposing the horizontal advection tendencies and the vertical velocity.

Preliminary tests showed that SCAM experiments are relevant for our purpose. We confirmed that we could reproduce the CAM results with the SCAM when forced with the hourly output of the CAM forecast run. We also checked the robustness of the solutions by assessing the sensitivity to small changes in the initial conditions. We showed that the collapse of the PBL in CAM is not sensitive to small variations in the initial conditions and is a robust feature in the SCAM simulations.

We assessed the impact of the vertical velocity on the PBL and cloud layer, by performing two types of experiments that are summarized in Table 4. In the first type (experiment WMEAN), we prescribed the daily mean vertical velocities at each vertical level and in the second type (experiment WDIURNAL), we added a mean diurnal cycle to the daily mean vertical velocities. The profiles of vertical velocity came from either CAM or ECMWF (denoted by the subscripts CAM or ECMWF). In order to isolate the effect of the vertical velocity, the horizontal advective tendencies of T and q were set to zero. The initialization and the prescribed forcing are identical in all the SCAM experiments, expect for the vertical velocity field.

Figure 8 shows the daily mean vertical velocity prescribed for the WMEAN experiments and the evolution of the specific humidity in these experiments. The vertical velocity profiles for CAM and ECWMF were extracted from the 3-day forecast starting on Oct 12, 2001. This date was chosen because the CAM forecast shows a clear collapse of the PBL while the PBL is maintained in the ECMWF forecast. The WMEAN experiments show that in the single-column model, the PBL is maintained when using the ECMWF vertical velocity profile and it collapses when using the CAM profile. The vertical velocity within the PBL itself plays a major role in the collapse or maintenance of the PBL in CAM. Below 900 mb, the vertical velocity is about twice as large in CAM than in the ECMWF model. The mean values are 15 mb/day (and 30mb/day) for the ECMWF (and CAM) models respectively. Switching the values of the vertical velocity below 900 mb between the prescribed vertical velocity profiles reverses the 2 behaviors: the PBL collapses when CAM omega is prescribed below 900 mb with ECWMF omega above and does not collapse with ECWMF omega prescribed below 900 mb and CAM omega above (not shown).

We also investigated the role of the diurnal cycle of omega in the cloud layer and PBL. In the WDIURNAL experiments, the prescribed vertical velocities are obtained by adding the diurnal cycle anomaly from Figure 7 to the daily mean vertical velocity profiles shown in Figure 8. Adding the diurnal cycle of omega does not have a significant impact on the LWP compared to the WMEAN experiment (not shown).

Our SCAM experiments show that the vertical velocity plays a major role in the collapse or maintenance of the PBL. If the amplitude of the vertical velocity reaches some threshold, the PBL collapses in CAM as it is the case for the 3-day forecast starting on Oct 12, 2001. However, this is a sufficient but not a necessary condition to the collapse of the PBL. In other forecasts, the PBL collapses even if the vertical velocity does not reach some threshold. We also observed in other stratocumulus regions that the collapse of the PBL can be due to non-local effects of the

vertical velocity (Hannay et al., 2005). In this case, the vertical velocity reaches a threshold in neighboring region and the effect is carried over by the large-scale advection. The vertical velocity is not the only player in the collapse of the PBL. Our simplified SCAM experiments did not allow identification of the other players.

5. Conclusions

Typically GCMs do not represent regions of stratocumulus well. The cloud amount tends to be underestimated in GCMs and the PBL height is too low compared to observations. In this study, we look at these processes using short-term forecasts covering the period of an in-situ experiment, the EPIC cruise of October 2001.

We examined two climate models (CAM and AM), one revised PBL scheme (CAM-UW) and one forecast model (ECMWF). A key problem common to all the models is that they produce too shallow PBLs. The observed PBL is about 1100 m depth while the models produce PBL heights between 400 and 800 m. The ECMWF forecast shows a steady PBL around 800-meter deep with no significant decrease or increase of the inversion height. The CAM and CAM-UW models unrealistically collapse the PBL depth within a 3-day forecast. The AM also shows some shallowing of the boundary layer depth, but less than is seen in CAM and CAM-UW forecasts. The LWP is underestimated in all the models except in the ECMWF model, which overestimates it. All the models produce a strong diurnal cycle in LWP but there are errors in the amplitude and the phase of the diurnal cycle compared to the EPIC observations. In particular, the AM and CAM-UW unrealistically decrease the LWP during the afternoon and this, in turn, affects the

radiative fluxes at the surface. There is a large spread in the surface energy budget terms amongst the models and large discrepancies with observational estimates.

We examined some of the reasons why the problem exists. We concluded that the vertical pressure velocity field is one of the aspect that has strong control over PBL depth and LWP. It is Not only the amplitude of the vertical pressure velocity field but also its vertical structure affect the collapse or the maintenance of the PBL. We also show that doubling of the vertical resolution in CAM has little impact on the simulation of the PBL.

This work illustrates how sensitive stratocumulus processes are to major forcing mechanisms and why it is so difficult to accurately represent clouds in GCMs. It also serves as a benchmark to measure improvements in future versions of the models.

Acknowledgements

The authors wish to thank Peter Caldwell from the University of Washington for providing an observational data compiled from a combination of measurements made during the EPIC 2001 stratocumulus field campaign. We are also grateful to Paquita Zuidema for providing LWP data and effective radius estimates. We also thank Ming Zhao and Sungsu Park for providing the AM and CAM-UW climatological data respectively. We thank John Truesdale for his support with the SCAM. We acknowledge the support of NSF ATM grant 0336688 for Cecile Hannay. Chris Bretherton was funded through NSF ATM grants 0336703 and 0433712. Stephen Klein is funded through the U. S. Department of Energy, Office of Science, Office of Biological and Environmental Research. The contribution of Stephen Klein was performed under the auspices of

the U. S. Department of Energy by Lawrence Livermore National Laboratory under contract DE-AC52-07NA27344. Jerry Olson and David Williamson were partially funded by the Office of Science (BER), U.S. Department of Energy, Cooperative Agreement No. DE-FC02-97ER62402.

References

Ahlgrimm, M. and D. A. Randall, 2006: Diagnosing Monthly Mean Boundary Layer Properties from Reanalysis Data Using a Bulk Boundary Layer Model. *Journal of Atmospheric Sciences*, **63,** 998-1012.

Bergman, J. W. and M. L. Salby, 1997: The Role of Cloud Diurnal Variations in the Time-Mean Energy Budget. *Journal of Climate*, **10,** 1114-1124.

Boville, B. A., P. J. Rasch, J. J. Hack, and J. R. McCaa, 2006: Representation of Clouds and Precipitation Processes in the Community Atmosphere Model Version 3 (CAM3). *Journal of Climate*, **19,** 2184-2198.

Boyle, J. S., D. Williamson, R. Cederwall, M. Fiorino, J. Hnilo, J. Olson, T. Phillips, G. Potter, and S. Xie, 2005: Diagnosis of Community Atmospheric Model 2 (CAM2) in numerical weather forecast configuration at Atmospheric Radiation Measurement sites. *Journal of Geophysical Research-Atmospheres*, **110,** D15516, doi: 10.1029/2004JD005109.

Bretherton, C. S. and S. Park, 2008: A New Moist Turbulence Parameterization in the Community Atmosphere Model. . *To be submitted to J. Geophys. Res.* .

Bretherton, C. S., T. Uttal, C. W. Fairall, S. E. Yuter, R. A. Weller, D. Baumgardner, K. Comstock, R. Wood, and G. B. Raga, 2004: The Epic 2001 Stratocumulus Study. *Bulletin of the American Meteorological Society*, **85,** 967-977.

Bushell, A. C. and G. M. Martin, 1999: The impact of vertical resolution upon GCM simulations of marine stratocumulus. *Climate Dynamics*, **15,** 293-318.

Caldwell, P., C. S. Bretherton, and R. Wood, 2005: Mixed-layer budget analysis of the diurnal cycle of entrainment in Southeast Pacific stratocumulus. *Journal of the Atmospheric Sciences*, **62,** 3775-3791.

Colbo, K., 2005: The IMET Sensor Accuracy. *Woods Hole Oceanographic Institution Upper Ocean Processes Group. Technical Note. [Available online at http://uop.whoi.edu/techdocs/TN05_09SensorAccuracy.pdf]*.

Collins, W. D., P. J. Rasch, B. A. Boville, J. J. Hack, J. R. McCaa, D. L. Williamson, B. P. Briegleb, C. M. Bitz, S.-J. Lin, and M. Zhang, 2006: The Formulation and Atmospheric Simulation of the Community Atmosphere Model Version 3 (CAM3). *Journal of Climate*, **19,** 2144-2161.

Collins, W. D., P. J. Rasch, B. A. Boville, J. J. Hack, J. R. McCaa, D. L. Williamson, J. T. Kiehl, B. Briegleb, C. Bitz, S.-J. Lin, M. Zhang, and Y. Dai, 2004: Description of the NCAR Community Atmosphere Model (CAM 3.0). *Technical Report NCAR/TN-464+STR, National Center for Atmospheric Research, Boulder, Colorado, National Center for Atmospheric Research, Boulder, Colorado, 210 pp. [Available online at http://www.ccsm.ucar.edu/models/atm-cam/docs/cam3.0/description/description.pdf]*

Duynkerke, P. G., S. R. de Roode, M. C. van Zanten, J. Calvo, J. Cuxart, S. Cheinet, A. Chlond, H. Grenier, P. J. Jonker, M. Kohler, G. Lenderink, D. Lewellen, C. L. Lappen, A. P. Lock, C. H. Moeng, F. Muller, D. Olmeda, J. M. Piriou, E. Sanchez, and I. Sednev, 2004: Observations and numerical simulations of the diurnal cycle of the EUROCS stratocumulus case. *Quarterly Journal of the Royal Meteorological Society*, **130,** 3269-3296.

Fairall, C. W. B., E. F.; Rogers, D. P.; Edson, J. B.; Young, G. S., 1996: Bulk parameterization of air-sea fluxes for Tropical Ocean-Global Atmosphere Coupled-Ocean Atmosphere Response Experiment. *Journal of Geophysical Research*, **101,** 3747-3764.

Garreaud, R., D, Mu, and R. oz, 2004: The Diurnal Cycle in Circulation and Cloudiness over the Subtropical Southeast Pacific: A Modeling Study. *Journal of Climate*, **17,** 1699-1710.

GFDL Global Atmospheric Model Development Team, 2004: The New GFDL Global Atmosphere and Land Model AM2-LM2: Evaluation with Prescribed SST Simulations. *Journal of Climate*, **17,** 4641-4673.

Hack, J. J., 1994: Parametrization of moist convection in the National Center for Atmospheric Research community climate model (CCM2). *Journal of Geophysical Research*, **99,** 5541-5568.

Hack, J. J. and J. A. Pedretti, 2000: Assessment of solution uncertainties in single-column modeling frameworks *Journal of Climate*, **13,** 352-365.

Hack, J. J., J. E. Truesdale, J. A. Pedretti, and J. C. Petch, 2004: SCAM User's Guide. *[Available on line at: http://www.ccsm.ucar.edu/models/atm-cam/docs/scam/]*.

Hack, J. J., J. M. Caron, S. G. Yeager, K. W. Oleson, M. M. Holland, J. E. Truesdale, and P. J. Rasch, 2006: Simulation of the Global Hydrological Cycle in the CCSM Community Atmosphere Model Version 3 (CAM3): Mean Features. *Journal of Climate*, **19,** 2199-2221.

Hannay, C., J. Kiehl, D. Williamson, J. Olson, and J. Hack, 2005: Forecast runs for the Pacific Cross-section**,** Low-Latitude Cloud Feedbacks Climate Process Team, Third Annual Meeting, 29-30 Nov. 2005, GFDL.

Holtslag, A. A. M. and B. A. Boville, 1993: Local Versus Nonlocal Boundary-Layer Diffusion in a Global Climate Model. *Journal of Climate*, **6,** 1825-1842.

Klein, S. A. and D. L. Hartmann, 1993: The seasonal cycle of low stratiform clouds. *Journal of Climate*, **6,** 1587-1606.

Klein, S. A., X. Jiang, J. Boyle, S. Malyshev, and S. Xie, 2006: Diagnosis of the summertime warm and dry bias over the U.S. Southern Great Plains in the GFDL climate model using a weather forecasting approach. *Geophys. Res. Lett*, **33,** L18805, doi:10.1029/2006GL027567.

Köhler, M., 2005: Improved prediction of boundary layer clouds. *ECMWF Newsletter*, **104,** [Available online at http://www.ecmwf.int/publications/newsletters/].

Lock, A. P., 2001: The Numerical Representation of Entrainment in Parameterizations of Boundary Layer Turbulent Mixing. *Monthly Weather Review*, **129,** 1148-1163.

Martin, G. M., D. W. Johnson, and A. Spice, 1994: The Measurement and Parameterization of Effective Radius of Droplets in Warm Stratocumulus Clouds. *Journal of the Atmospheric Sciences*, **51,** 1823-1842.

Moorthi, S. and M. J. Suarez, 1992: Relaxed Arakawa-Schubert. A Parameterization of Moist Convection for General Circulation Models. *Monthly Weather Review*, **120,** 978-1002.

Onogi, K., J. Tsutsui, H. Koide, M. Sakamoto, S. Kobayashi, H. Hatsushika, T. Matsumoto, N. Yamazaki, H. Kamahori, K. Takahashi, S. Kadokura, K. Wada, K. Kato, R. Oyama, T. Ose, N. Mannoji, and R. Taira, 2007: The JRA-25 Reanalysis. *J. Meteor. Soc. Japan*, **85,** 369-432.

Park, S. and C. S. Bretherton, 2008: Impact of the University of Washington moist turbulence and shallow convection schemes on climate simulations with the Community Atmosphere Model. *To be submitted to J. Geophys. Res*.

Phillips, T. J., G. L. Potter, D. L. Williamson, R. T. Cederwall, J. S. Boyle, M. Fiorino, J. J. Hnilo, J. G. Olson, S. Xie, and J. J. Yio, 2004: Evaluating Parameterizations in General

Circulation Models: Climate Simulation Meets Weather Prediction. *Bulletin of the American Meteorological Society*, **85,** 1903-1915.

Pope, V. D., J. A. Pamment, D. R. Jackson, and A. Slingo, 2001: The Representation of Water Vapor and Its Dependence on Vertical Resolution in the Hadley Centre Climate Model. *Journal of Climate*, **14,** 3065-3085.

Rasch, P. J. and J. E. Kristjansson, 1998: A Comparison of the CCM3 Model Climate Using Diagnosed and Predicted Condensate Parameterizations. *Journal of Climate*, **11,** 1587-1614.

Rotstayn, L. D., B. F. Ryan, and J. J. Katzfey, 2000: A Scheme for Calculation of the Liquid Fraction in Mixed-Phase Stratiform Clouds in Large-Scale Models. *Monthly Weather Review*, **128,** 1070-1088.

Rozendaal, M. A., C. B. Leovy, and S. A. Klein, 1995: An Observational Study of Diurnal Variations of Marine Stratiform Cloud. *Journal of Climate*, **8,** 1795-1809.

Schubert, W. H., J. S. Wakefield, E. J. Steiner, and S. K. Cox, 1979: Marine Stratocumulus Convection. Part I: Governing Equations and Horizontally Homogeneous Solutions. *Journal of the Atmospheric Sciences*, **36,** 1286-1307.

Siebesma, A. P., C. Jakob, G. Lenderink, R. A. J. Neggers, J. Teixeira, E. van Meijgaard, J. Calvo, A. Chlond, H. Grenier, C. Jones, M. Köhler, H. Kitagawa, P. Marquet, A. P. Lock, F. Müller, D. C. Olmeda, and C. Severijns, 2004: Cloud representation in general-circulation models over the northern Pacific Ocean: A EUROCS intercomparison study. *Quarterly Journal of the Royal Meteorological Society*, **130,** 3245-3267.

Stevens, B., D. H. Lenschow, G. Vali, H. Gerber, A. Bandy, B. Blomquist, J. L. Brenguier, C. S. Bretherton, F. Burnet, T. Campos, S. Chai, I. Faloona, D. Friesen, S. Haimov, K. Laursen, D. K.

Lilly, S. M. Loehrer, S. P. Malinowski, B. Morley, M. D. Petters, D. C. Rogers, L. Russell, V. Savic-Jovcic, J. R. Snider, D. Straub, M. J. Szumowski, H. Takagi, D. C. Thornton, M. Tschudi, C. Twohy, M. Wetzel, and M. C. van Zanten, 2003: Dynamics and Chemistry of Marine Stratocumulus - DYCOMS-II. *Bulletin of the American Meteorological Society*, **84,** 579-593.

Sundqvist, H., 1988: Parameterization of condensation and associated clouds in models for weather prediction and general circulation simulation. *Physically-based Modeling and Simulation of Climate and Climate Change, Vol. 1, edited by M. E. Schlesinger, Kluwer Academic***,** 433-461.

Tiedtke, M., 1989: A Comprehensive Mass Flux Scheme for Cumulus Parameterization in Large-Scale Models. *Monthly Weather Review*, **117,** 1779-1800.

——, 1993: Representation of Clouds in Large-Scale Models. *Monthly Weather Review*, **121,** 3040-3061.

Tompkins, A. M., P. Bechtold, A. C. M. Beljaars, A. Benedetti, S. Cheinet, M. Janisková, M. Köhler, P. Lopez, and J.-J. Morcrette, 2004: Moist physical processes in the IFS: Progress and Plans *ECMWF Technical Memoranda*, **452,** [Available online at http://www.ecmwf.int/publications/library/do/references/list/14].

Uppala, S. M., Kållberg, P.W., Simmons, A.J., Andrae, U., da Costa Bechtold, V., Fiorino, M., Gibson, J.K., Haseler, J., Hernandez, A., Kelly, G.A., Li, X., Onogi, K., Saarinen, S., Sokka, N., Allan, R.P., Andersson, E., Arpe, K., Balmaseda, M.A., Beljaars, A.C.M., van de Berg, L., Bidlot, J., Bormann, N., Caires, S., Chevallier, F., Dethof, A., Dragosavac, M., Fisher, M., Fuentes, M., Hagemann, S., Hólm, E., Hoskins, B.J., Isaksen, L., Janssen, P.A.E.M., Jenne, R., McNally, A.P., Mahfouf, J.-F., Morcrette, J.-J., Rayner, N.A., Saunders, R.W., Simon, P., Sterl, A., Trenberth, K.E., Untch, A., Vasiljevic, D., Viterbo, P., and Woollen, J. , 2005: The ERA-40 re-analysis. *Quart. J. R. Meteorol. Soc.*, **131,** 2961-3012.doi:10.1256/qj.04.176.

Williamson, D. L. and J. G. Olson, 2007: A comparison of forecast errors in CAM2 and CAM3 at the ARM Southern Great Plains Site. *Journal of Climate*, **20,** 4572-4585.

Williamson, D. L., J. Boyle, R. Cederwall, M. Fiorino, J. Hnilo, J. Olson, T. Phillips, G. Potter, and S. C. Xie, 2005: Moisture and temperature balances at the Atmospheric Radiation Measurement Southern Great Plains Site in forecasts with the Community Atmosphere Model (CAM2). *Journal of Geophysical Research-Atmospheres*, **110,** D15S16, doi: 10.1029/2004JD005109.

Wood, R., 2006: Relationships between optical depth, liquid water path, droplet concentration, and effective radius in adiabatic layer cloud. *Personal note. [Available online at http://www.atmos.washington.edu/~robwood]*.

Wood, R. and C. S. Bretherton, 2004: Boundary Layer Depth, Entrainment, and Decoupling in the Cloud-Capped Subtropical and Tropical Marine Boundary Layer. *Journal of Climate*, **17,** 3576-3588.

Wood, R., C. S. Bretherton, and D. L. Hartmann, 2002: Diurnal cycle of liquid water path over the subtropical and tropical oceans. *Geophysical Research Letters*, **29,** 2092, doi:10.1029/2002GL015371.

Zhang, G. Z. and N. A. McFarlane, 1995: Sensitivity of Climate Simulations to the Parameterization of Cumulus Convection in the Canadian Climate Centre General Circulation Model. *Atmosphere-Ocean*, **33,** 407-446.

Zuidema, P. and D. L. Hartmann, 1995: Satellite Determination of Stratus Cloud Microphysical Properties. *Journal of Climate*, **8,** 1638-1657.

Zuidema, P., E R Westwater, C Fairall, and D. Hazen, 2005: Ship-based liquid water path estimates in marine stratocumulus. *J. Geophys. Res.*, **110,** D20206, doi:10.1029/2005JD005833.

List of Figures

Figure 8: The upper panel shows the daily mean vertical velocity used in the experiment WMEAN. The lower panels show the evolution of the specific humidity (g kg-1) in the WMEANECMWF experiment (left panel) and in the WMEANCAM experiment (right panel).

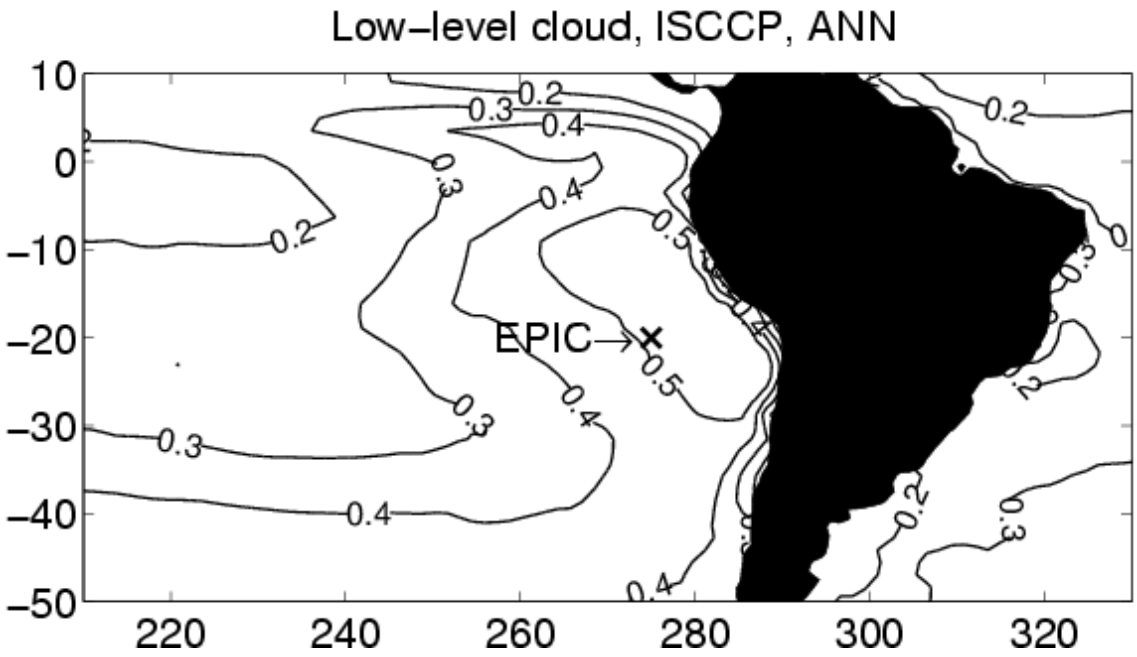

Figure 1: The EPIC point (20S-85W) is located in a region of persistent stratocumulus off the coast of South America. The contours are the annual low-level clouds from ISCCP.

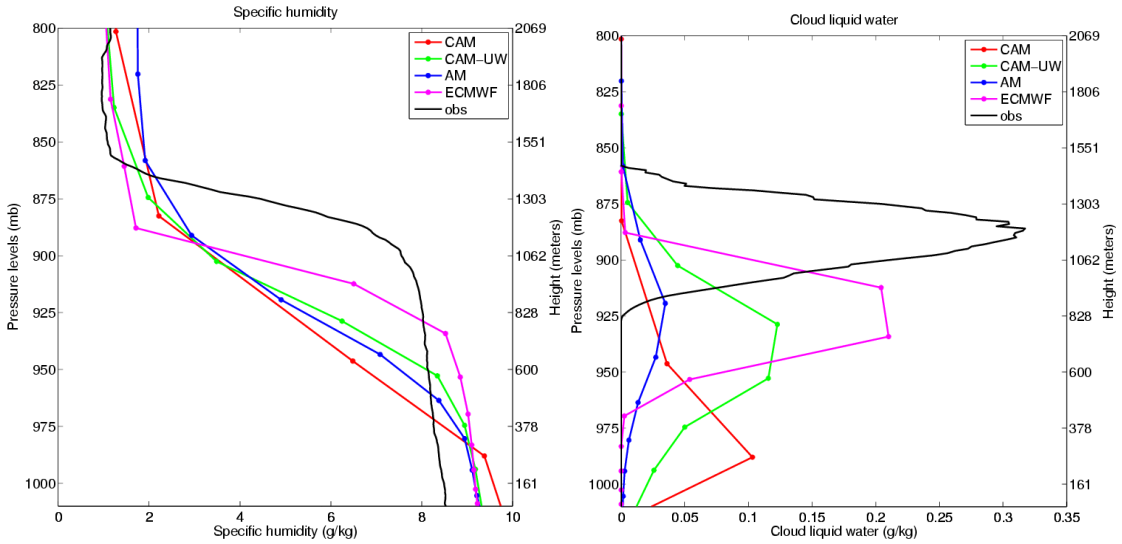

Figure 2: Comparison of the 6-day observed mean specific humidity and cloud liquid water profiles from EPIC observations with the mean from the ECMWF analysis created by cycle 29r1 for the same period and location and with October climatological profiles for CAM, CAM-UW and AM interpolated at the EPIC point.

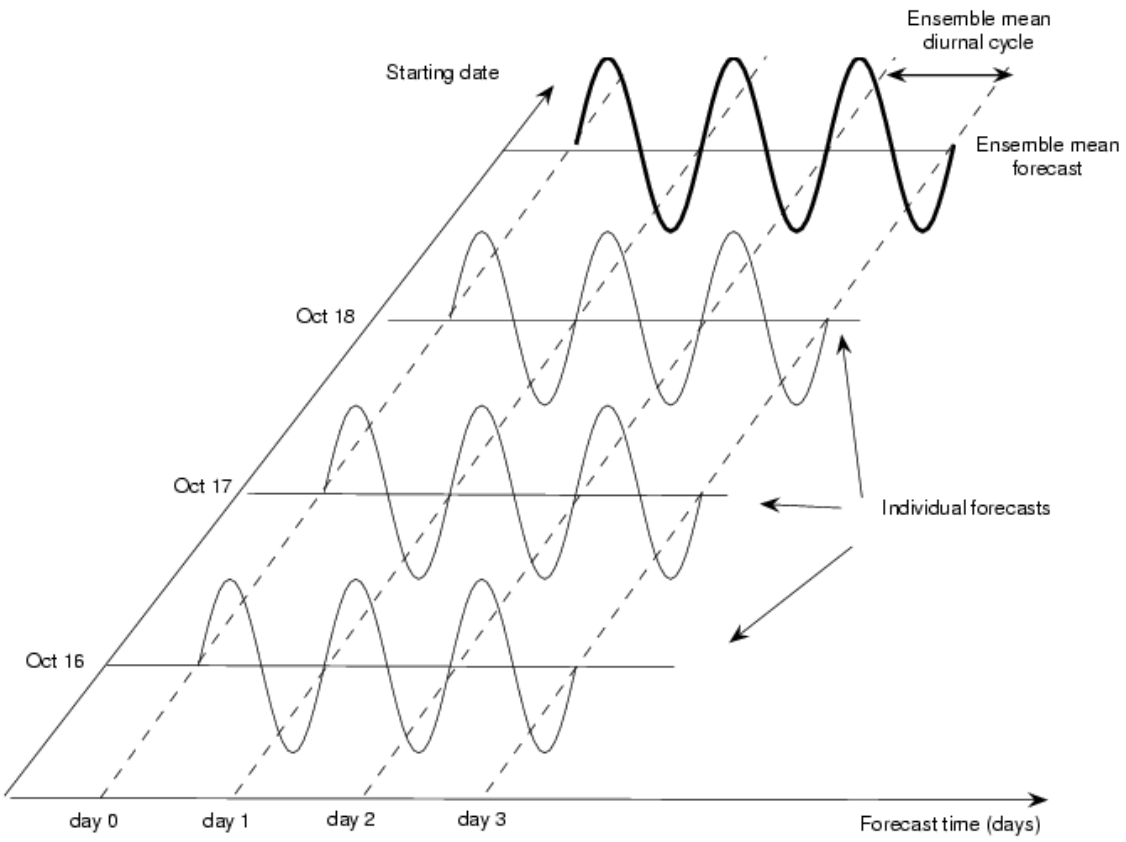

Figure 3: Ensemble mean forecast (bold line) taken along the dash line.

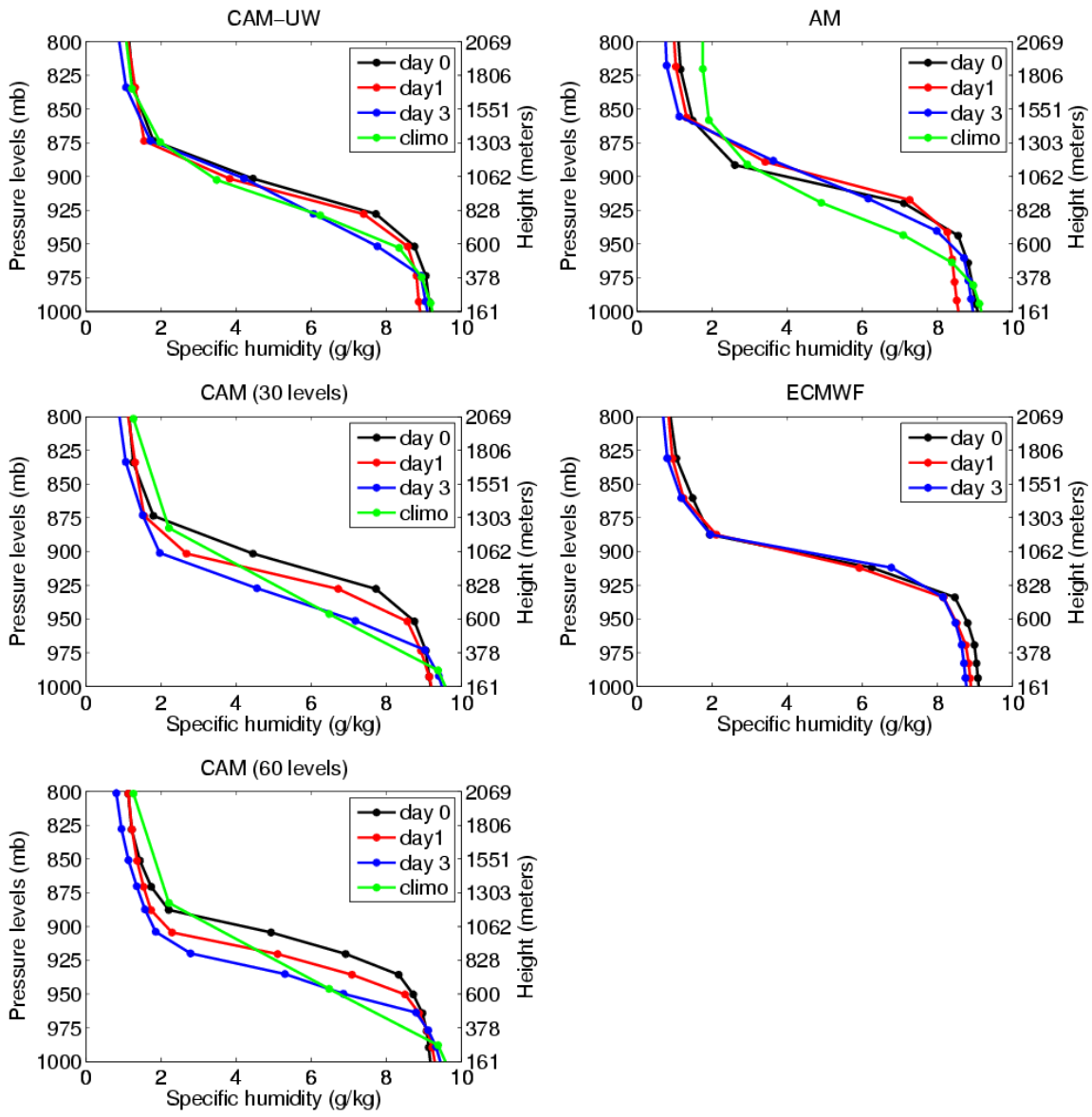

Figure 4 : Ensemble mean forecast and climatological specific humidity for CAM, CAM-UW, AM and ECMWF. Forecasted specific humidity at day 0, day 1 and day 3 (black, red, blue). Mean climate specific humidity for October climatology (green). Notice that the forecasts for CAM are on 30 levels and 60 levels and the climatology is on 26 levels for the reasons developed in section 2.1.

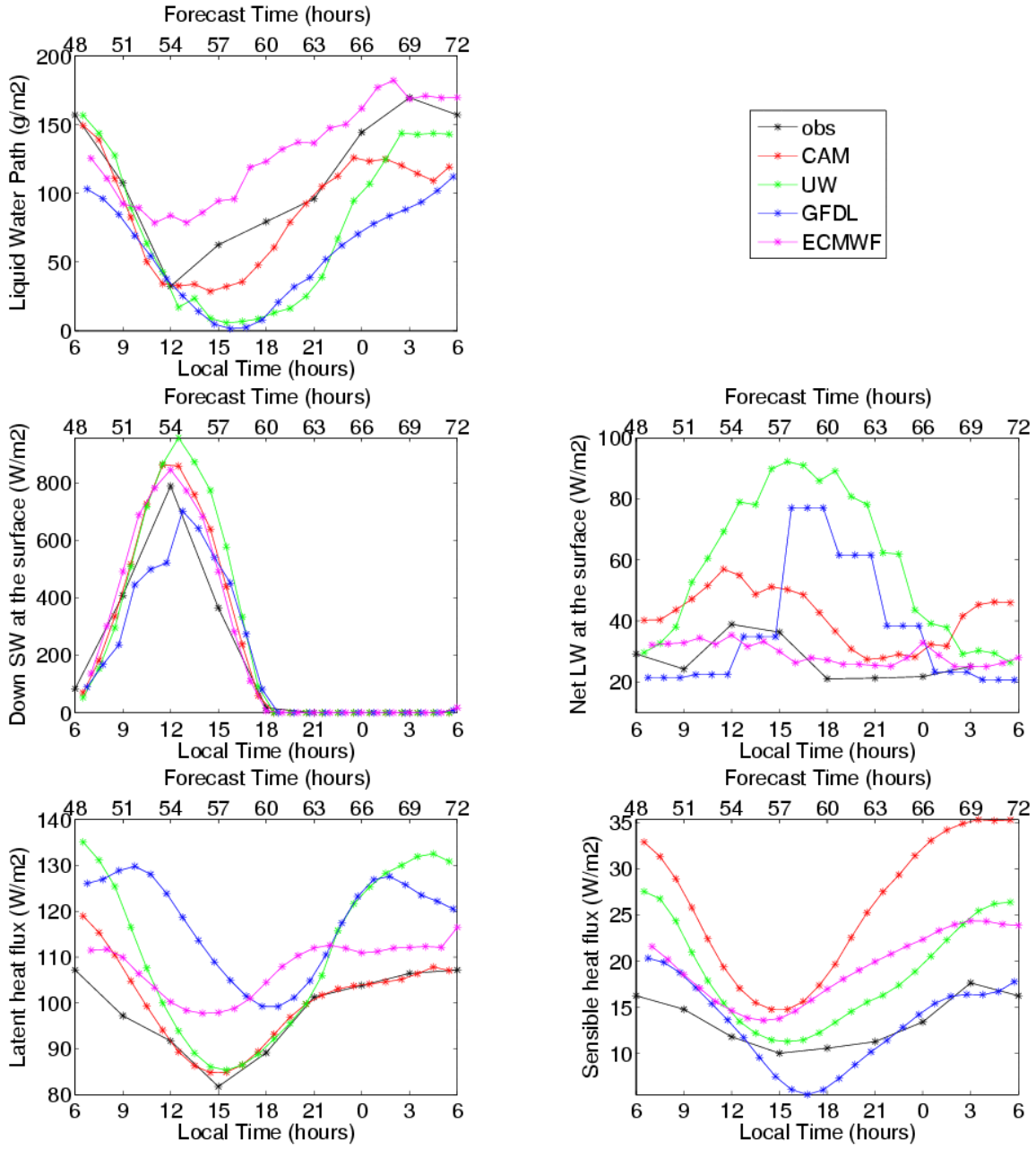

Figure 5: Diurnal cycle of the ensemble mean forecast (day 3) of the LWP, downwelling shortwave radiation, net longwave radiation, latent heat flux and sensible heat flux.

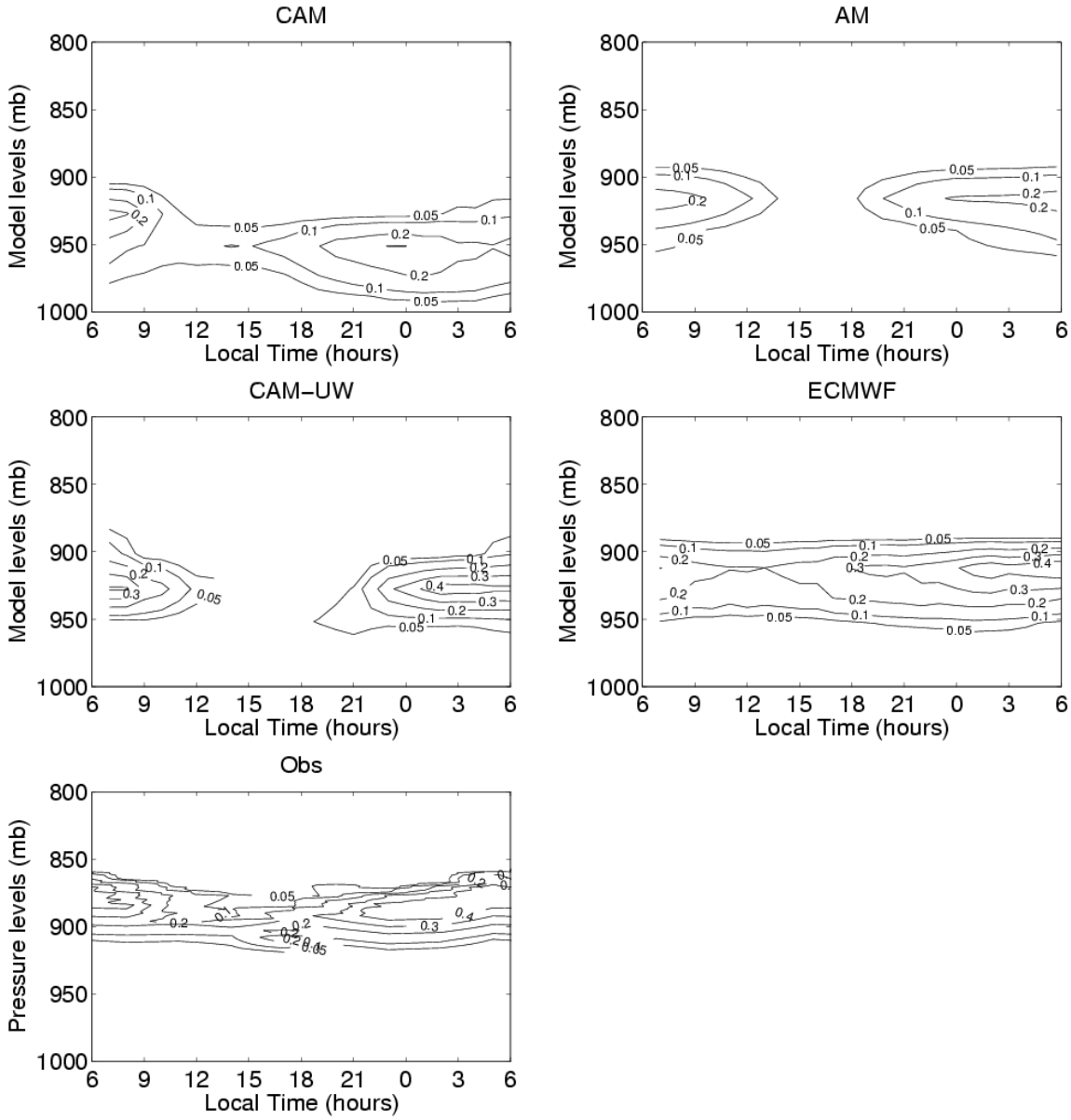

Figure 6: Diurnal cycle of the ensemble mean forecast (day 3) of liquid cloud water.

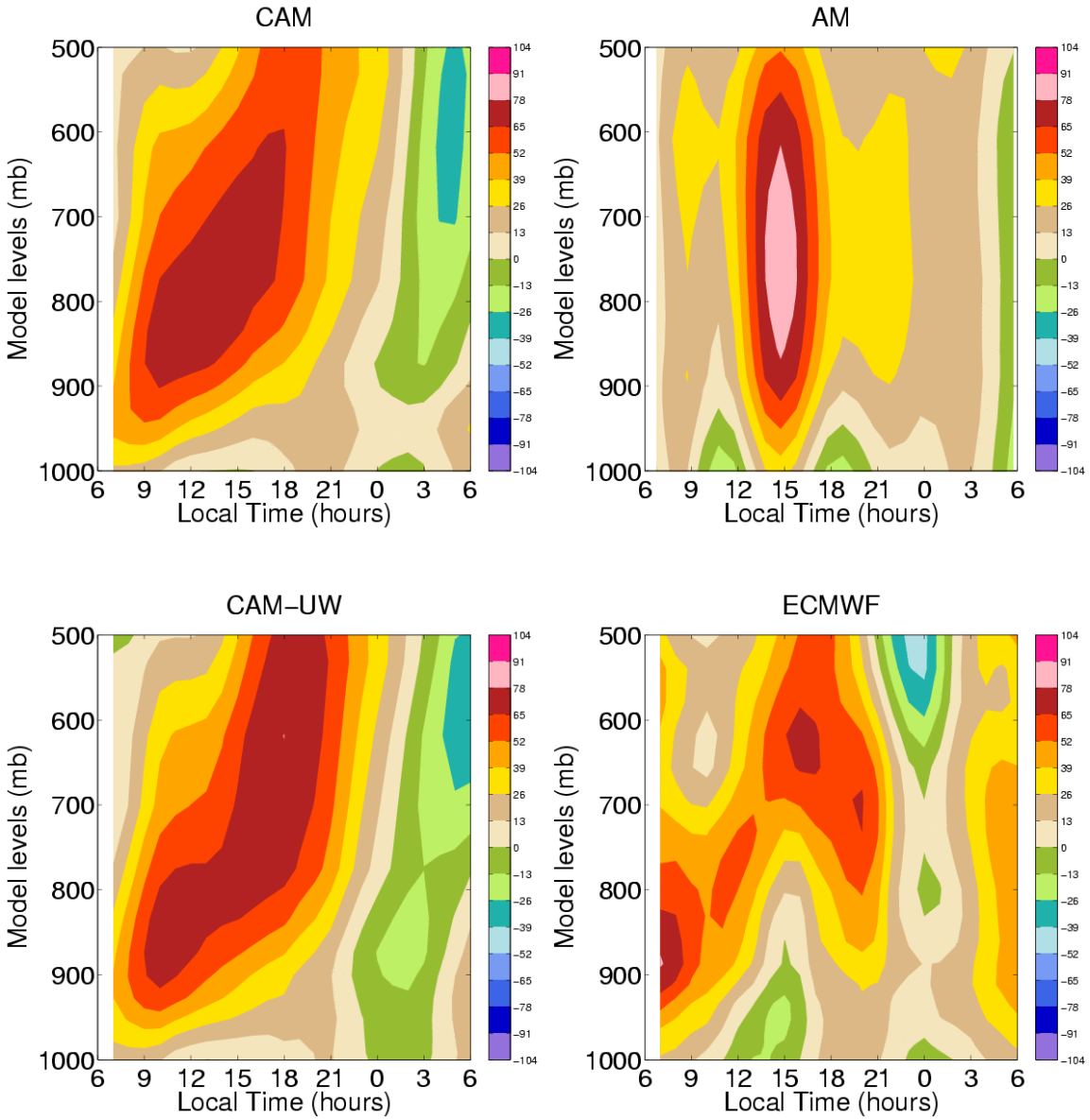

Figure 7: Diurnal cycle of the ensemble mean forecast (day 3) of the pressure vertical velocity.

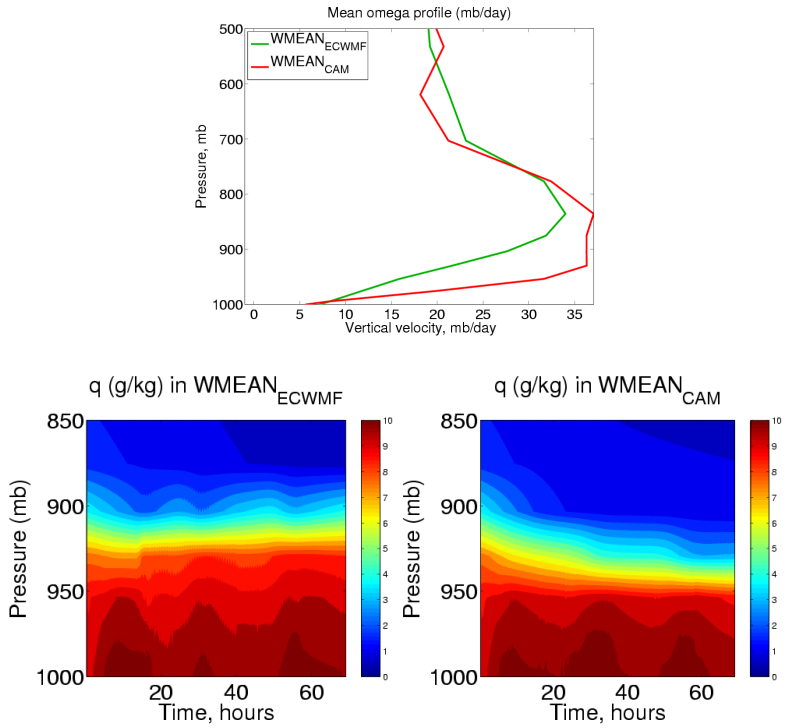

Figure 8: The upper panel shows the daily mean vertical velocity used in the experiment WMEAN. The lower panels show the evolution of the specific humidity (g kg^{-1}) in the $WMEAN_{ECMWF}$ experiment (left panel) and in the $WMEAN_{CAM}$ experiment (right panel).

List of Tables

Table 1: Physical parameterization of the models

Parameterization	CAM	CAM-UW	AM	ECMWF
Deep convection	Zhang and McFarlane (1995)	Same as CAM	Relaxed Arakawa-Schubert (Moorthi and Suarez, 1992)	Tiedtke (1989)
Shallow convection	Hack (1994)	Park and Bretherton (2008)	Relaxed Arakawa-Schubert (Moorthi and Suarez, 1992)	Tiedtke (1989)
PBL	Holtslag and Boville (1993)	Bretherton and Park (2008)	Lock (2001) scheme modified for stratocumulus-top entrainment for the PBL	Köhler (2005)
Clouds	Sundqvist (1988) and Rasch and Kristjansson (1998)	Same as CAM	Macrophysics from Tiedtke (1993) Microphysics from Rotstayn et al. (2000)	Tiedtke (1993)

Table 2: Model vertical and horizontal resolutions and number of levels in the lowest 1.5km of the troposphere.

	CAM	CAM-UW	AM	ECMWF
Horizontal resolution	T42 (~2.8 x 2.8 degree)	T42 (~2.8 x 2.8 degree)	2 x 2.5 degree	T511 (~0.35 x 0.35 degree)
Vertical resolution	26 levels (climate) 30 levels (forecast) 60 levels (forecast)	30 levels	24 levels	60 levels
Number of levels in the lowest 1.5 km	4 (26-level resolution) 7 (30-level resolution) 12 (60-level resolution)	7	8	12

Table 3: Daily average of the LWP, effective radius, optical depth and the surface energy budget terms. The numbers in parentheses shows typical errors in the daily estimates of observed values (see Zuidema et al., 2005 for LWP and Colbo, 2005 for the surface fluxes). The lower value of the observed effective radius was estimated assuming an adiabatic cloud layer and the larger value from MODIS. The observed net shortwave radiation was computed from the downwelling component assuming a surface albedo equal to 0.05.

	LWP ($g\ m^{-2}$)	Re (microns)	Net SW ($W\ m^{-2}$)	Net LW ($W\ m^{-2}$)	Latent heat ($W\ m^{-2}$)	Sensible heat ($W\ m^{-2}$)	Net flux ($W\ m^{-2}$)
Observations	106(6)	13-17	-208(4)	28 (6)	98 (5)	14 (1.5)	-68 (8)
CAM	87	14	-221	40	102	26	-53
CAM-UW	75	14	-243	57	113	19	-54
AM	57	6.7	-179	37	118	12	-12
ECMWF	131	12.4	-214	29	107	19	-59

Table 4: Summary of the SCAM experiments. Two types of experiments were performed. The daily mean vertical velocities at each vertical level are prescribed in the WMEAN experiment, and a mean diurnal cycle is added to the daily mean vertical velocities in the WDIURNAL experiment. The profiles of vertical velocity came from either CAM or ECMWF (subscript CAM or ECMWF).

	Use daily mean profile	Use mean daily cycle profile
Use CAM vertical velocity	$WMEAN_{CAM}$	$WDIURNAL_{CAM}$
Use ECMWF vertical velocity	$WMEAN_{ECWMF}$	$WDIURNAL_{ECWMF}$